Author Manuscript

Author Manuscript

Author Manuscript

Author Manuscript

HHS Public Access

Author manuscript

Neurochem Int. Author manuscript; available in PMC 2016 July 15.

Published in final edited form as:

Neurochem Int. 2012 April ; 60(5): 506–516. doi:10.1016/j.neuint.2012.02.007.

NR2A and NR2B subunits differentially mediate MAP kinase signaling and mitochondrial morphology following excitotoxic insult

Anthony M. Choo[1], **Donna M. Geddes-Klein**[1], **Adam Hockenberry**, **David Scarsella**, **Mahlet N. Mesfin**, **Pallab Singh**, **Tapan P. Patel**, and **David F. Meaney**[*]

Department of Bioengineering, University of Pennsylvania, Philadelphia, PA, USA

Abstract

NMDA receptors are essential for neurotransmission and key mediators of synaptic signaling, but they can also trigger deleterious degenerative processes that lead to cell death. Growing evidence suggests that selective blockade of the heterogeneous subunits that comprise the NMDA receptor may enable better control of pharmacotherapies for treating neurological diseases and injuries. We investigated the relationship between NMDAR activation, MAPK signaling, and mitochondrial shape following an excitotoxic insult. NR2A- and NR2B-containing NMDARs differentially mediated acute changes in cytosolic calcium, alterations in mitochondrial morphology, and phosphorylation of the MAPKs ERK and JNK. Activation of NR2A-containing NMDARs was associated with JNK phosphorylation that was neuroprotective in neuronal cultures subjected to excitotoxicity. In contrast, activation of NR2B-containing NMDARs triggered calcium accumulation in mitochondria that was strongly associated with mitochondrial swelling and neuronal cell death. Indeed, while blockade of NR2B-containing receptors was neuroprotective, this protection was lost when NR2A-initiated JNK phosphorylation was inhibited. Given the modest selectivity of the NR2A inhibitor, NVP-AAM077, the results highlight the significance of the relative, rather than absolute, activation of these two NMDA subtypes in modulating cell death pathways. Therefore, the balance between concurrent activation of NR2B-containing and NR2A-containing NMDARs dictates neuronal fate following excitotoxicity.

Keywords

NMDA receptor; Calcium; JNK; ERK; Mitochondria

1. Introduction

NMDA receptors are key glutamate receptors mediating many important neuronal functions including plasticity, regeneration, and survival (Hardingham and Bading, 2010). The

[*]Corresponding author. Address: Department of Bioengineering, 240 Skirkanich Hall, 210 S. 33rd Street, Philadelphia, PA 19104-6321, USA. Tel.: +1 215 573 2726; fax: +1 215 573 2071., dmeaney@seas.upenn.edu (D.F. Meaney).

[1]These authors contributed equally to this study.

Conflict of interest

Authors declare no conflict of interest.

Author Manuscript Author Manuscript Author Manuscript Author Manuscript

molecular diversity of the subunits forming NMDA receptors is well described, with different subunit combinations appearing in distinct brain regions (Monyer et al., 1994). The diversity of these subunit combinations makes the pharmacological control of NMDA receptors complex, yet offers the possibility for the selective blockade of a specific subpopulation of NMDA receptors to better control both the desired effects and deleterious consequences of NMDAR directed therapies in neurological disease and injury (Faden et al., 1988; Waxman and Lynch, 2005).

Previous work shows the activation of different NMDAR subpopulations plays an influential role in determining if NMDA receptor activation elicits either pro-survival or apoptotic signaling (Hardingham et al., 2002). Activation of extrasynaptic (NR1/NR2B) NMDA receptors leads to a calcium influx into the mitochondria; this preferred involvement of the mitochondria suggests that the stimulation of NR2B-containing NMDARs is a strong signal for neuronal apoptosis (Bonfoco et al., 1995; Hardingham et al., 2002; Liu et al., 2007). Alternatively, activation of NR2A-containing NMDARs located at the synapse provides a prosurvival stimulus, and using this preferred receptor activation strategy can even precondition cultured neurons to withstand glutamate insult that would normally cause neuronal death (Soriano et al., 2006) or to remove the mechanosensitivity of the NMDAR (Geddes-Klein et al., 2006). Clearly, balancing the competing roles of NMDAR subpopulation activation and inhibition is an intriguing and potentially effective approach for developing NMDAR directed therapies for neurological disease.

Three key areas are emerging for understanding the role of NMDA receptor activation on neuronal fate. Local scaffolding of proteins with the NMDAR is one key regulatory point, where the interaction of the NR2B C-terminus with PSD-95 is critical for the activation of nitric oxide mediated signaling; interrupting the interaction will lead to improved outcome following ischemic brain injury (Cui et al., 2007; Gascon et al., 2008). A second key regulatory point is the potential preferred routing of calcium to the mitochondria following extrasynaptic NMDA receptor activation, which may be partly attributed to the distinct calcium buffering capabilities of synaptic and nonsynaptic mitochondria (Brown et al., 2006; Naga et al., 2007). The impact of this preferred routing of calcium, though, is less clear. A final regulatory point is the connection between signaling within NMDA receptor microdomains and gene expression, which activate signaling networks that lead to nuclear changes and influence neuronal survival (Bading et al., 1995; Hardingham et al., 2001).

In this study, we consider the relative consequences of preferred stimulation of NR2B and, alternatively, NR2A-containing NMDARs on both mitogen activated protein kinase (MAPK) signaling and mitochondria morphology. Our overall objective was to understand the relative balance of these two distinct pathways on neuronal survival. Consistent with previous reports, we show NMDA stimulation leads to a rapid and persistent change in mitochondria morphology. The alterations in mitochondria morphology are dependent upon NR2B-containing NMDAR activation, and we find both synaptic and extrasynaptic NR2B-containing NMDARs contribute to the change in mitochondrial morphology that is triggered by NMDA receptor stimulation. Although we find no significant role for stimulation of NR2A-containing NMDARs on mitochondrial morphology, we did observe a rapid and sustained activation of c-jun N-terminal kinase (JNK) from the preferred activation of

Author Manuscript Author Manuscript Author Manuscript Author Manuscript

NR2A-containing NMDARs. Interestingly, we find that blocking JNK activation will erase any neuroprotection conferred by blocking NR2B-containing NMDARs during an NMDA exposure. Together, these data show that the selection of strategies to target NMDAR subpopulations for improving neuronal survival after excitotoxicity relies on key signaling steps mediated by both NR2A- and NR2B-containing NMDARs.

2. Materials and methods

2.1. Cell culture

Primary cortical neurons were isolated from embryonic day 18 rodents, as previously described (Geddes-Klein et al., 2006). Briefly, embryos (E17–E19) were removed by caesarean section from a timed-pregnant Sprague–Dawley rat and the cortices were removed. Tissue was digested in trypsin/DNase at 37 °C, centrifuged (1000*g* × 5 min), and filtered to derive a cell suspension. Dissociated cortical neurons were plated onto glass dishes with Neurobasal medium (Invitrogen, Carlsbad, CA) plus B-27 serum-free supplement, GlutaMAX-I supplement, 0.025 mM L-glutamic acid, 50–100 U of penicillin, and 50–100 μg of streptomycin all from Invitrogen). Cells were grown in an incubator at 37 °C and 5% CO_2 in Neurobasal medium with B-27 Serum-free supplement and GlutaMAX-I supplement (Feeding Medium). Cultures were treated with AraC (1 μM, Sigma) starting at DIV 4 and continuing until DIV 8 to minimize glial contamination of the cultures. Past work shows this culturing process yields >90% neurons in the cultures (Lusardi et al., 2004). Unless otherwise noted, cultures were tested 17–19 DIV after plating.

2.2. Drug treatments

For excitotoxic injuries, neurons were treated with NMDA in magnesium-free saline for up to 1 h. The following drug treatments were diluted in HEPES buffered saline (final concentration noted in parentheses): *N*-methyl-D-aspartic acid (NMDA) (Sigma; 30– 100 μM), Ro 25-6981 (Sigma; 20 μM), APV (D(−)-2-Amino-5-phosphonopentanoic acid; Sigma; 50 μM), NVP (NVP-AAM077) (generously provided by Yves Auberson, Novartis, Basel, Switzerland; 500 nM), MK801 ((+)-MK-801 hydrogen maleate; Sigma, 10 μM), bicuculline (50 μM, Sigma), SP600125 (20 μM, EMD Biosciences). In conditions using Ru360, a mitochondrial calcium uniporter inhibitor, we carefully adhered to the preparation methods outlined in earlier studies to maintain activity and minimize compound oxidation (Johnson et al., 2002), preparing the solution under nitrogen to a stock concentration of 10 mM. Nitrogen gas in an enclosed chamber was bubbled through water and buffered saline to remove oxygen. After reconstitution, aliquots of Ru360 were added to deoxygenated HEPES-buffered saline to 10 μM. Aliquots were kept on ice and wrapped with parafilm and foil. Aliquots were only thawed once, as Ru360 loses significant activity after additional freeze-and-thaw cycles. For control experiments, vehicle saline was applied alone or with pharmacological blockers without NMDA.

2.3. Measuring mitochondrial morphology

Primary neurons were transfected with Mito*e*YFP protein overnight the day before imaging. The mitochondrially targeted *e*YFP construct (generously provided by Dr. Ian J. Reynolds, University of Pittsburgh, Pittsburgh, PA) consists of the gene for *e*YFP, inserted into the

Author Manuscript Author Manuscript Author Manuscript Author Manuscript

mammalian expression vector pCDNA3 (Invitrogen). The construct was complexed with Lipofectamine 2000 (Invitrogen) with a reagent-to-plasmid ratio of 3:2. The complex was incubated in Dulbecco's Modified Eagle Medium (BioWhittaker, Basel, Switzerland) at room temperature for 20 min before it was added to the cells. Transfected cells were then incubated in Neurobasal medium (without any supplements) for 4 h at 37 °C and 5% CO_2 before the media was replaced with feeding medium. Cells were ready for use the following day, and the *e*YFP tag allowed for a determination of mitochondrial morphology. On average, approximately 10% of the cells in a culture were successfully transfected.

Images of the mitochondria were either collected prior to and following NMDA stimulation, or every 10 s for a total of 10 min. In time lapse experiments, NMDA was added to the media approximately 3 min into the imaging sequence. In both protocols, images were collected using appropriately filtered excitation light, using a Hamamatsu C4742-95 digital camera.

2.4. Analysis of mitochondria shape

Each mitochondrion in an image was identified manually, and the outline of the mitochondrion was automatically identified using an adaptive threshold algorithm (Nikolaidis and Pitas, 2001) which accommodates for variation in the local background fluorescence of each mitochondria. A shape index parameter (SI) was identified for each mitochondrion:

$$\mathrm{SI}=\mathrm{maximum}\,(L/W) \quad (1)$$

where L is the maximum length and W the maximum width of the outlined mitochondrion. We defined the difference in the shape index as the difference between the shape of each mitochondrion prior to and following stimulation:

$$\Delta\mathrm{SI}=\mathrm{SI}_{\mathrm{final}}-\mathrm{SI}_{\mathrm{initial}} \quad (2)$$

Normally, mitochondria in dendrites often assume a long tubular shape (SI > 1) that can change to nearly spherical following NMDA stimulation (SI ~ 1). Therefore, negative values for ΔSI indicate a contraction and swelling of mitochondria. Mitochondria were quantified from 2 to 21 cultures in each treatment group with an average of $N = 75$ ΔSI measurements per condition.

2.5. Calcium imaging

Cytosolic calcium levels were measured with the calcium sensitive fluorescent dye, Fura-2, as previously described (Geddes-Klein et al., 2006). Briefly, neurons were incubated in 5 μm fura-2AM for 40 min at 37 °C, 5% CO_2. Following incubation, neurons were rinsed three times with saline (120 mM NaCl, 5.4 mM KCl, 0.8 mM $MgCl_2$, 1.8 mM $CaCl_2$, 25 mM HEPES, 15 mM glucose). Cells were excited alternately at 340 and 380 nm and an image of the emission (510 nm) from each excitation wavelength was collected using a Hamamatsu C4742-95 digital camera (Universal Imaging, West Chester, PA, USA) attached to a Nikon

Author Manuscript Author Manuscript Author Manuscript Author Manuscript

TE300 microscope. Images were collected every 10 s. In all experiments, baseline data were recorded prior to NMDA stimulation and emission intensity was monitored continuously for 1 h following NMDA application. The emission intensity images were analyzed on an individual neuron basis to calculate changes in the emission intensity ratio (F_{340}/F_{380}) for each neuron in the field of view. All cells within the field of view were analyzed for each experiment. All experiments were performed at room temperature.

To measure calcium uptake by mitochondria, 500 nM Rhod-2 was applied to cortical neurons for 15 min. After rinsing twice with HEPES-buffered saline supplemented with 10 μM glycine, the neurons were either incubated in HEPES-buffered saline for immediate use or inhibitor for 5 min prior to testing. Rhod-2 fluorescence was measured (560 nm excitation; 630 nm emission) using images captured every 5 s for a period of 10 min. Mitochondrial fluorescence change was detected by monitoring the fluorescence intensity of individual pixels in a digitized field containing neuronal processes. Using MetaMorph 7.1.3.0 software (Molecular Devices, Downingtown, PA), individual mitochondria were captured as regions of interest (ROI) using *e*YFP images as a guide; the resulting ROIs were then analyzed for changes in fluorescence of Rhod-2. The relative change in the fluorescence of the ROI from the initial fluorescence captured in the first image (F_o) was used as a measure of mitochondrial calcium (Babcock et al., 1997). To avoid single frame bias in the data set, an average of ten images post-NMDA application was divided by the average of ten images pre-NMDA application was considered the change in fluorescence of each ROI, representing a single mitochondrion. The mean fluorescence change of each mitochondrion from 2 to 14 cultures was compiled to calculate the group means.

2.6. Cell viability

Cell viability was assessed by measuring LDH secreted into the media from 5 to 9 cultures per treatment group, according to the manufacturer's instructions (CytoTox-ONE™ Homogeneous Membrane Integrity Assay, Promega).

2.7. Western blotting

Cortical neurons were washed 3 times with saline and harvested in lysis buffer (10 mM HEPES, pH 7.4, 200 mM NaCl, 30 mM EDTA, 0.5% TritonX-100, 0.5 mM sodium orthovanadate, COMPLETE mini Protease Inhibitor (Roche, Indianapolis, IN)). Cell lysates (3–6 samples per group) were centrifuged at 16,000*g* for 15 min at +4 °C; supernatants were then collected and stored at −80 °C.

Lysates were loaded in 4–12% Bis-Tris gels (Invitrogen Corp., Carlsbad, CA) and were resolved at 200 V for 1 h. After gel electrophoresis, proteins were transferred to a PVDF membrane (Invitrogen Corp., Carlsbad, CA) at a constant voltage of 10 V overnight (12 h) in 1X transfer buffer (Invitrogen Corp., Carlsbad, CA) containing 20% methanol. Membranes were blocked in 5% dry milk containing 20 mM Tris–HCl (pH 7.4), 1.5 M NaCl, 0.1% Tween-20. The blots were then incubated with primary antibodies for the total JNK (Cell Signaling, #9252, 1:500), phosphorylated JNK (Cell Signaling, #9251, 1:500), ERK (Promega, V114A, 1:3000), phosphorylated ERK (Cell Signaling, 4376S, 1:500), or actin (Chemicon; MAB1501, 1:1000). Following incubation with primary antibodies overnight at

Author Manuscript Author Manuscript Author Manuscript Author Manuscript

+4 °C, blots were incubated with horseradish peroxidase conjugated secondary antibodies (1:2000; Jackson Immuno- Research, West Grove, PA) for 2 h at room temperature. Enhanced chemiluminescence (Perkin Elmer, Boston, MA) reagents were used to visualize the immunoreactivity on X-ray film. Separate protein bands were quantified (42 and 44 kDa separately for ERK; 46 and 54 kDa separately for JNK) with a computer assisted two-dimensional densitometric scanning (Kodak 1D Image Analysis Software, Eastman Kodak Company, Rochester, NY). The densitometric readings of phosphorylated proteins were normalized to their corresponding total protein bands.

2.8. Statistics

Shape change measurements developed from time lapse images of mitochondrial morphology and relative changes in Rhod-2 fluorescence were analyzed using a one-way ANOVA, followed by Tukey posthoc testing. Cell viability in response to NMDA stimulation was assessed by two-way ANOVA (NMDAR antagonist vs. NMDA application) with Tukey posthoc testing. Cell viability in the presence of SP600125 JNK inhibitor was assess by one-way ANOVA followed by Dunnett's posthoc test to compare NMDA receptor antagonism to SP600125 treatment without NMDA stimulation. The relative increase in ERK and JNK phosphorylation was analyze with one-way ANOVA at each time-point followed by Dunnett's test to compare the individual level of phosphorylation to a common baseline control without NMDA stimulation. Differences between NMDAR antagonists were analyzed with two-way ANOVA (NMDAR antagonist vs. time) followed by Tukey posthoc testing. Differences were considered significant at $P < 0.05$. All data are presented as mean ± SEM.

3. Results

3.1. Excitotoxicity

We first established experimental conditions that would activate both NR2B and NR2A-containing NMDA receptors. Several features of culturing conditions can influence the timing of expression, localization, and relative composition of NR2A and NR2B-containing NMDARs in cortical neurons. Therefore, we tested our cultures directly with NMDA stimulation to assess the timing and relative amount of calcium loading that occurs under different pharmacological conditions (Fig. 1A). Following a dose of NMDA (100 μM) capable of activating NR1/NR2A, NR1/NR2A/NR2B and NR1/NR2B NMDAR combinations, three distinct phases of cytosolic calcium increases occurred over 45 min: (1) an initial peak typically within 1–2 min after the start of NMDA stimulation (peak normalized ratio = 4.3 ± 0.6), (2) a subsequent modest recovery that would reduce cytosolic calcium levels over the next 3–5 min by approximately 25% (minimum normalized ratio = 3.2 ± 0.4), and (3) a longer term gradual accumulation of cytosolic calcium that would continue for the duration of time used in monitoring cytosolic calcium (peak normalized ratio = 6.0 ± 1.0). The initial increase and partial recovery of cytosolic calcium could be attributed to the preferred activation of NR2A-containing NMDARs, as it was prevented with NVP-AAM077 pre-treatment. In comparison, the delayed and gradual accumulation of cytosolic calcium is influenced by NR1/NR2B NMDARs, as this component was eliminated with pre-treatment of cultures with ifenprodil. A similar relative reduction in the peak

Author Manuscript Author Manuscript Author Manuscript Author Manuscript

normalized ratio was observed when using Ro 25-6981, an antagonist with higher preferential affinity for the glutamate binding site on NR2B subunit (data not shown).

With this ability to manipulate the activation of different NMDAR subpopulations, we next tested if there were different neuronal survival outcomes among these different stimulation protocols. Past work shows the relative role of NR2A and NR2B-containing NMDARs on pathology, with several cited mechanisms that can contribute to these unique outcomes (Hardingham et al., 2002; von Engelhardt et al., 2007). When assessing cell death after NMDA stimulation, we observed a statistically significant interaction between NMDAR antagonists and the application of an excitotoxic dose of NMDA ($P = 0.008$). Tukey posthoc analysis showed our NMDA stimulation protocol led to an increase in cell death (47 ± 12%, $P = 0.015$ compared to untreated, Fig. 1B) 24 h following the stimulation as assessed by the release of lactate dehydrogenase (LDH). Cell death was virtually eliminated when neurons were pretreated with the NR2B antagonist Ro 25-6981 (3 μM, 8 ± 5%, $P = 0.999$ compared to Ro 25-6981 treatment without NMDA, $P = 0.031$ compared to NMDA treatment without antagonists). In comparison, though, pre-treatment with NVP-AAM077 (500 nM) still triggered significant cell death ($P = 0.001$ compared to NVPAAM077 alone) following excitotoxic NMDA stimulation, and rather, slightly exacerbated excitotoxicity (62 ± 11% in NVP-AAM077 treated vs. 47 ± 12% with NMDA alone).

3.2. Activation of MAP kinases

Recent studies suggest different NMDAR subpopulations are critical for activating some, but not all, members of the MAPK cascade and can therefore play an influential role on neuronal survival signaling. Under this model of NMDA-mediated neuronal death, we first examined if two members of the MAPK family involved in neuronal survival and death (ERK and JNK) were phosphorylated following NMDA stimulation directed towards either NR2B-containing or NR2A-containing NMDARs. Consistent with previous studies, we observed rapid ERK activation following 100 μMNMDA (Fig. 2A–C). Phosphorylation of 44 kDa ERK was elevated by 2.4 ± 0.4-fold above baseline levels by 15 min following NMDA insult (Fig. 2B, $P = 0.005$ 44 kDa pERK/ERK at 15 min NMDA vs. untreated baseline). Phosphorylation of 42 kDa ERK progressively increased over the course of the 60 min to 2.4 ± 0.3-fold above baseline p42 ERK levels (Fig. 2C, $P = 0.001$ 42 kDa pERK/ERK at 60 min NMDA vs. untreated baseline).

Two-way ANOVA showed a significant difference between NMDA receptor antagonist on 44 kDa ERK phosphorylation after NMDA stimulation ($P = 0.006$ main effect of antagonist). Antagonism of NR2B-containing NMDA receptors accelerated the phosphorylation of 44 kDa ERK (Fig. 2B, NMDA + ifenprodil at 5 min 44 kDa pERK/ERK = 2.9 ± 0.4-fold, $P < 0.001$ compared to untreated baseline) whereas antagonism of NR2A-containing NMDA receptors prevented significant elevation in 44 kDa ERK phosphorylation above baseline levels ($P > 0.2$ NMDA + NVP-AAM077 at all times vs. untreated baseline). The effect of preferential antagonism of NR2A-and NR2B-containing NMDA receptors on 42 kDa ERK phosphorylation was similar to that observed for the 44 kDa isoform, though, the relative changes in phosphorylation was more modest (Fig. 2C).

Author Manuscript Author Manuscript Author Manuscript Author Manuscript

A second member of the MAPK family associated with neuronal fate is the c-jun N-terminal kinase (JNK), which is activated following ischemia, traumatic injury to the brain and spinal cord, and excitotoxic injury (Borsello et al., 2003). NMDA stimulation did not trigger a statistically significant difference in 54 kDa JNK phosphorylation over the course of 60 min ($P = 0.251$ main effect of NMDA antagonism). In contrast, two-way ANOVA indicated a significant effect of NMDA antagonism on activation of 46 kDa JNK (Fig. 2F, $P = 0.021$ main effect of NMDA antagonism). NVP-AAM077 prevented significant elevation of 46 kDa JNK phosphorylation compared to NMDA treatment alone ($P = 0.012$ Tukey posthoc comparison NMDA vs. NVP-AAM077 pooled over time). In comparison to baseline phosphorylation levels, NMDA stimulation increased 46 kDa JNK phosphorylation by 1.5 ± 0.2-fold ($P = 0.003$ NMDA at 60 min vs. untreated baseline). Similar to ERK phosphorylation, antagonism of NR2B-containing receptors with ifenprodil resulted in an earlier increase in 46 kDa JNK phosphorylation (Fig. 2F, $P = 0.004$ NMDA + ifenprodil at 15 min vs. untreated baseline).

Given this specific activation of 46 kDa JNK mediated by NR2A-containing NMDARs, we next assessed if this activation could influence neuronal fate, as detected by LDH release 24 h after NMDA stimulation (Fig. 2G). We used the same NMDA stimulation protocol that was sufficient to produce a significant LDH release 24 h after stimulation. NMDA stimulation in the presence of the JNK inhibitor SP600125 still triggered significant cell death (38 ± 6% in SP600125 with NMDA-treated cultures, $P < 0.001$ compared to SP600125 controls). As before, preferred antagonism of NR2A-containing NMDA receptors did not prevent significant cell death (57 ± 10%, $P < 0.001$ SP600125 + NVP-AAM077 + NMDA vs. SP600125 without NMDA). Interestingly, antagonism of NR2B-containing receptors with Ro 25-6981 was no longer protective in the presence of SP600125 (38 ± 14% in Ro 25-6981 + SP600125 + NMDA treated cultures, $P = 0.002$ vs. SP600125 without NMDA). These data suggests that modest JNK phosphorylation may contribute to the neuroprotection afforded by inhibition of NR2B-containing NMDARs.

3.3. Mitochondrial morphology

To this point, our data showed activation of NR2B-containing NMDARs are important for causing neuronal death, and that early MAPK signaling is an important mediator for the neuroprotection offered by blocking NR2B-containing NMDARs. Next, we focused on the proximal step of NR2B-NMDAR activation, considering if the mitochondria are involved as a downstream regulator of NR2B-NMDAR activation. Several past reports suggest that NMDA stimulation will lead to an accumulation of mitochondrial calcium and the rounding of mitochondrial shape (Peng and Greenamyre, 1998; Rintoul et al., 2003). Normally, mitochondria exist as long tubular organelles throughout the dendrites (Fig. 3A–C). Similar to previous reports, we found that NMDA stimulation caused a rapid change in mitochondrial morphology throughout the dendrites (Fig. 3D–F), with these stimulated neurons showing a much more rounded mitochondria profile within 2 min of NMDA stimulation ($\Delta SI = -1.61 \pm 0.09$). Remarkably, only brief periods of NMDA stimulation were necessary to induce long lasting changes in mitochondria shape, as changes in shape caused by only 5 min of NMDA stimulation lasted for at least 1 h following the removal of the stimulus (Fig. 3G).

Author Manuscript Author Manuscript Author Manuscript Author Manuscript

We tested the potential contributing roles of NMDAR subpopulations on the measured change in mitochondria shape in 17–19 DIV cortical neurons (Fig. 4). Although broad spectrum NMDAR antagonism with MK801 prevented any mitochondrial shape change (ΔSI = −0.16 ± 0.1; NS compared to untreated controls), application of an NR2A-preferred antagonist (NVP-AAM077) prior to NMDA stimulation did not prevent the swelling of mitochondria (ΔSI = −1.42 ± 0.13; $P < 0.01$ compared to untreated; NS compared to NMDA). In contrast, the NR2B antagonist Ro 25-6981 significantly reduced the change in mitochondria shape that was caused by NMDA stimulation (ΔSI = −0.61 ± 0.09; $P < 0.01$ compared to NMDA treatment). The change in mitochondrial shape in the presence of Ro 25-6981, however, was still greater than in untreated controls ($P = 0.04$) indicating that non-NR1/NR2B NMDARs also contribute to the change in mitochondrial shape. To discriminate the relative role of synaptic and extrasynaptic NMDARs on the resulting changes in mitochondrial morphology more specifically, we used a combined bicuculline and MK-801 treatment protocol to induce action potential bursting thereby enabling MK-801 to specifically block synaptic NMDARs (Hardingham et al., 2002). The bursting induced by bicuculline, a $GABA_A$ receptor antagonist, only slightly altered mitochondrial shape (data not shown). Applying NMDA to these treated cultures activates only extrasynaptic NMDARs (Hardingham et al., 2002) which was sufficient to trigger significant swelling of mitochondria (ΔSI = −2.03 ± 0.28; $P < 0.01$ compared to untreated controls, NS compared to NMDA).

Given the discussion in the literature on the relative composition of NMDARs at synaptic and extrasynaptic sites during the maturation of cultures in vitro (Thomas et al., 2006), we also evaluated mitochondrial swelling in 11–14 DIV cortical neurons (Fig. 4H). Similar to our results in mature neurons, swelling of mitochondria was not significantly attenuated by blocking NR2A-containing NMDARs with NVP-AAM077 (ΔSI = −1.06 ± 0.28; $P = 0.01$ compared to untreated, NS compared to NMDA), whereas the NR2B antagonist Ro 25-6981 attenuated the change in mitochondria shape that was triggered by NMDA stimulation (ΔSI = −0.41 ± 0.25; NS compared to untreated controls). Young and mature cultures differed in their response to NMDA when synaptic receptors were blocked with the combined bicuculline and MK-801 treatment. In contrast to mature cultures, extrasynaptic activation in young cultures did not trigger a robust change in mitochondrial shape (ΔSI = −0.38 ± 0.13; NS compared to untreated; $P < 0.01$ compared to NMDA). These results are consistent with a decrease in fraction of NR2B-containing NMDARs that appear at the synapse in more mature neurons.

3.4. Calcium accumulation in mitochondria

Finally, we considered if this mitochondria shape change was linked directly to accumulation of mitochondrial calcium following NMDA stimulation. We studied the role of receptor subtype composition in the accumulation of mitochondrial calcium, as the role of receptors subtype composition on mitochondrial swelling was consistent across culture age (Fig. 4). Given this similarity among culture age, we focused our studies on 11–14 DIV neurons. Using a calcium sensitive fluorescent dye (Rhod-2) that accumulates in the mitochondria, we found NMDA stimulation led to a rapid increase in average Rhod-2 fluorescence (Fig. 5A and B, $F/F_0 = 1.33 \pm 0.02$; $P < 0.01$ relative to untreated controls). We

Author Manuscript Author Manuscript Author Manuscript Author Manuscript

could block this increase in Rhod-2 fluorescence entirely with APV pre-treatment (F/F_0 = 1.05 ± 0.01; NS relative to untreated controls), while the relative fluorescence increased using NVP-AAM077 pre-treatment (Fig. 5C and D, F/F_0 = 1.55 ± 0.05; $P < 0.01$ relative to untreated controls). In comparison, inhibiting NR1/NR2B NMDARs with Ro 25-6981 led to a significant reduction in mitochondrial Rhod-2 fluorescence that was not significantly different from untreated controls (Fig. 5E and F, F/F_0 = 1.06 ± 0.02).

Increased activity of the mitochondrial calcium uniporter (Starkov et al., 2004) is one potential mechanism of mitochondrial calcium regulation. To this end, pre-treatment with Ru360 prevented any significant increase in mitochondrial calcium after NMDA stimulation (Fig. 6A and B, F/F_0 = 1.06 ± 0.02). Interestingly, blockade of NR2A-containing NMDARs and pre-treatment with Ru360 showed a slight increase in mitochondrial calcium (Fig. 6C, F/F_0 = 1.14 ± 0.02, P = 0.08 vs. untreated controls). This is likely associated with the significant enhancement in mitochondrial calcium elevation caused by NVP treatment alone (Fig. 5G). In parallel with the attenuation of mitochondrial calcium accumulation, treatment with Ru360 also prevented the mitochondrial swelling that was triggered by NMDA stimulation (Fig. 6D–F).

4. Discussion

In this report, we examine the relationship between NMDAR activation, MAPK signaling, and mitochondrial changes on neuronal fate following an excitotoxic insult. Importantly, our data suggests that the relative activation of NR2A and NR2B NMDAR subtypes is sufficient to induced distinct patterns of cytosolic calcium accumulation, JNK-phosphorylation, acute pathologic mitochondrial morphology, and cell death. We show that preferential blockade of NR2A-containing NMDARs reduces 46 kDa JNK phosphorylation, and that blockade of JNK phosphorylation abolished the neuroprotection afforded by antagonism of NR2B subunits in neuronal cultures subjected to excitotoxicity. We show activation of NR1/NR2B NMDARs are important for triggering changes in mitochondrial morphology and influencing neuronal fate, and there is a strong association between mitochondrial calcium accumulation and swelling. Therefore, the balance between the relative activation of NR2B-containing and NR2A-containing NMDARs contribute to neuronal fate following excitotoxicity.

A limiting factor in this study was the use of the only modestly selective NR2A inhibitor, NVP-AAM077 (Berberich et al., 2005; Frizelle et al., 2006; Neyton and Paoletti, 2006; Weitlauf et al., 2005). NVP-AAM077 displays greater than 100-fold preferential blockade of NR2A- versus NR2B-containing receptors in human recombinant NMDA receptors (Auberson et al., 2002). In rodent recombinant receptors, the selectivity is significantly reduced—on the order of 10-fold with glutamate agonist and 20-fold with NMDA as the agonist (Frizelle et al., 2006). Indeed, at the dose used in this study (500 nM), NVP-AAM077 significantly attenuates all NR1/NR2A and approximately 50% of the NR1/NR2B NMDARS expressed in HEK293 cells, with an unknown inhibition of the triheteromeric NR1/NR2A/NR2B NMDA receptors (Bartlett et al., 2007). However, despite the off-target blockade of NR2B-containing receptors, we still observed a unique response profile in neurons treated with NVP-AAM077 compared to either NR2B inhibition with Ro 25-6981

Author Manuscript Author Manuscript Author Manuscript Author Manuscript

or total NMDA inhibition with APV. Namely, preferential antagonism of NR2A-containing NMDA receptors with NVP-AAM077 was consistently different than antagonism of NR2B-containing NMDA receptors with respect to neuronal viability, MAPK activation, and excitotoxic changes in mitochondrial morphology. Moreover, we observed consistent changes in mitochondrial morphology when testing mature neurons (17–19 DIV) with a protocol to isolate the extrasynaptic receptors, which are predominantly NR1/NR2B subtypes at this age in culture (Monyer et al., 1994; Thomas et al., 2006). Therefore, we feel these data provide a meaningful insight into discriminating between NR2B- and NR2A-containing NMDARS.

The role of glutamate on changing the morphology of neuronal mitochondria is well described (Rintoul et al., 2003). Similar to previous studies, we find that NMDA exposure can cause a rapid swelling of mitochondria, and that this swelling response is irreversible after only 5 min of NMDA treatment. Although past studies showed that the loss of mitochondrial membrane potential and increase in mitochondrial calcium occurs by activating NR2B-containing NMDARs (Hardingham et al., 2002), our data is the first to show a direct association between NR2B-NMDAR activation, calcium accumulation in the mitochondria, and mitochondrial swelling in cultured neurons. Inhibiting NR2A-containing NMDARs enhanced the accumulation of mitochondrial calcium, despite the reduction in cytosolic calcium, during NMDA treatment. One possible reason for this relative increase in mitochondrial calcium is a shunting of calcium to extrasynaptic mitochondria, further illustrating the significance of distinct routes of calcium influx as mentioned by Tymianski and colleagues (Sattler et al., 1998). An additional factor that could explain this enhancement in mitochondrial calcium is the relative buffering ability of synaptically localized and non-synaptic mitochondria. In vitro assays show that synaptic mitochondria have a reduced ability to buffer large amounts of calcium when compared to non-synaptic mitochondria (Brown et al., 2006; Naga et al., 2007). As a result, preferred activation of NR2B-containing NMDARs would increase the calcium directed to nonsynaptic mitochondria and therefore lead to a relative increase in mitochondrial calcium load. This calcium buffering characteristic of synaptic mitochondria may also explain how a modest increase in mitochondrial calcium occurs in younger cultures when only the NR2A-containing NMDARs are activated. Together, these data suggest that both the intrinsic properties of the mitochondria and selective activation of different NMDAR sub-populations contribute to the calcium signaling and response to NMDA exposure.

These data add to the emerging picture of the role of NMDAR subunit composition and pathways that can regulate neuronal survival. Considerable recent discussion shows the developmental expression and localization of NR2B-containing NMDARs in primary neurons, with evidence showing relatively immature cultures have a large fraction of NR2B-containing NMDARs appearing at the synapse, as well as extrasynaptic locations (von Engelhardt et al., 2007). A recent paper shows that this developmental expression of NMDAR subunits influences the relative role of NR2B-containing NMDARs on mitochondrial calcium accumulation, and this role becomes more complex in more mature (21–28 DIV) cultures (Stanika et al., 2009). In our data, blocking synaptically localized NMDA receptors did not prevent swelling of mitochondria in mature (17–19 DIV) cultures, thereby indicating that the effect of NMDA on mitochondrial morphology was dominated by

Author Manuscript Author Manuscript Author Manuscript Author Manuscript

NR2B-containing, extrasynaptic NMDAR stimulation. In younger cultures, where we expect more NR2B-containing NMDARs at the synapse, blocking synaptically localized NMDARs reduced mitochondrial swelling. Together these data suggest that NR2B-containing NMDARs can trigger mitochondrial swelling from both synaptic and extrasynaptic domains. Given recent evidence that NMDA receptors may traffic laterally between synaptic and extrasynaptic domains (Harney et al., 2008; Zhao et al., 2008), the interaction between NMDA receptor subtypes and their localization will need to be further elucidated in order to optimize an NMDAR sub-type directed neuroprotective strategy.

As an initial strategy to blunt the effects of NMDA toxicity, a reasonable approach would be to block the receptor subpopulations most responsible for mitochondrial morphology changes. We find excellent neuroprotection by blocking the NR2B-containing NMDARs in maturing neurons, consistent with several previous studies (DeRidder et al., 2006; Liu et al., 2007; von Engelhardt et al., 2007). Given the numerous reports examining the role of JNK in mediating neuronal death (Philpott and Facci, 2008), though, it may be surprising that our data show JNK phosphorylation is important for sustaining neuroprotection following the blockade of NR2B-containing NMDARs. One must consider, however, the possible contribution of the different JNK isoforms in mediating the neuroprotection response (Bjorkblom et al., 2008; Waetzig et al., 2006). Recent work with transgenic mice shows that JNK 1 knockout mice exhibit a significant increase in lesion volume deficit following an ischemic injury, suggesting that JNK 1 plays an important role in neuronal survival (Brecht et al., 2005). Similarly, activation of JNK 1/2 plays a significant role in survival of cerebellar granule neurons exposed to the NR2B agonist quinolinic acid. In comparison, JNK3 knockout mice show significant attenuation of neurological deficits following ischemia and excitotoxic brain injury (Pirianov et al., 2007; Yang et al., 1997). Hence, although JNK signaling has been associated with neurodegeneration (Borsello et al., 2003; Yang et al., 1997), they also play crucial roles in neuroprotection and regeneration (Haeusgen et al., 2009; Waetzig et al., 2006). Commercially available antibodies for phosphorylated JNK do not distinguish well among phosphorylated JNK 1/2/3 due to their extensive homology (Haeusgen et al., 2009), and therefore our data do not allow us to determine whether the JNK phosphorylation caused by NMDA stimulation is preferentially targeted to one or more isoforms. In addition, although SP600125 continues to be used ubiquitously to inhibit JNK phosphorylation (Bogoyevitch and Arthur, 2008), there is some evidence that other kinases may also be affected (Bain et al., 2003) and hence these off target effects may also modulate neuronal survival in response to differential NR2A and NR2B subunit activation. Future work using either targeted knockdown or overexpression techniques would better define the exact role of each isoform in mediating the neuroprotection offered by NR2B-based antagonists.

In summary, our data add to the emerging information on the complex roles that NMDARs play on both survival and degenerative processes in neurons. Changes in the mitochondria morphology are influenced strongly by the dependence of NR2B-containing NMDARs and neuronal maturity, and likely play a strong role in the neuronal death following NMDA toxicity, but our data also suggest that cellular signaling activated during a common receptor specific antagonist approach (NR2B-NMDAR inhibition) also plays an important downstream role in sustaining the neuroprotection afforded by NMDAR antagonists in

Author Manuscript Author Manuscript Author Manuscript Author Manuscript

maturing cultures. These data highlight that combined therapies may be more complex than simply adding one neuroprotective therapy with another, as the combined effect may not be as effective as originally intended. With the emerging role of combined therapies in clinical disorders, these data highlight complex factors for consideration in future studies.

Acknowledgments

This work was supported by NIH Grants NS35712 and HD41699. The technical assistance of Dr. Gang Lu, Dr. Gul Serbest, and Kimberly Schiffman is gratefully acknowledged.

References

Auberson YP, Allgeier H, Bischoff S, Lingenhoehl K, Moretti R, Schmutz M. 5-phosphonomethylquinoxalinediones as competitive NMDA receptor antagonists with a preference for the human 1A/2A, rather than 1A/2B receptor composition. Bioorg Med Chem Lett. 2002; 12:1099–1102. [PubMed: 11909726]

Babcock DF, Herrington J, Goodwin PC, Park YB, Hille B. Mitochondrial participation in the intracellular Ca^{2+} network. J Cell Biol. 1997; 136:833–844. [PubMed: 9049249]

Bading H, Segal MM, Sucher NJ, Dudek H, Lipton SA, Greenberg ME. *N*-methyl-D-aspartate receptors are critical for mediating the effects of glutamate on intracellular calcium concentration and immediate early gene expression in cultured hippocampal neurons. Neuroscience. 1995; 64:653–664. [PubMed: 7715778]

Bain J, McLauchlan H, Elliott M, Cohen P. The specificities of protein kinase inhibitors: an update. Biochem J. 2003; 371:199–204. [PubMed: 12534346]

Bartlett TE, Bannister NJ, Collett VJ, Dargan SL, Massey PV, Bortolotto ZA, Fitzjohn SM, Bashir ZI, Collingridge GL, Lodge D. Differential roles of NR2A and NR2B-containing NMDA receptors in LTP and LTD in the CA1 region of two-week old rat hippocampus. Neuropharmacology. 2007; 52:60–70. [PubMed: 16904707]

Berberich S, Punnakkal P, Jensen V, Pawlak V, Seeburg PH, Hvalby O, Kohr G. Lack of NMDA receptor subtype selectivity for hippocampal long-term potentiation. J Neurosci. 2005; 25:6907–6910. [PubMed: 16033900]

Bjorkblom B, Vainio JC, Hongisto V, Herdegen T, Courtney MJ, Coffey ET. All JNKs can kill, but nuclear localization is critical for neuronal death. J Biol Chem. 2008; 283:19704–19713. [PubMed: 18474608]

Bogoyevitch MA, Arthur PG. Inhibitors of c-Jun N-terminal kinases-JuNK no more? Biochim Biophys Acta, Proteins Proteomics. 2008; 1784:76–93.

Bonfoco E, Krainc D, Ankarcrona M, Nicotera P, Lipton SA. Apoptosis and necrosis: two distinct events induced, respectively, by mild and intense insults with *N*-methyl-D-aspartate or nitric oxide/superoxide in cortical cell cultures. Proc Natl Acad Sci USA. 1995; 92:7162–7166. [PubMed: 7638161]

Borsello T, Clarke PG, Hirt L, Vercelli A, Repici M, Schorderet DF, Bogousslavsky J, Bonny C. A peptide inhibitor of c-Jun N-terminal kinase protects against excitotoxicity and cerebral ischemia. Nat Med. 2003; 9:1180–1186. [PubMed: 12937412]

Brecht S, Kirchhof R, Chromik A, Willesen M, Nicolaus T, Raivich G, Wessig J, Waetzig V, Goetz M, Claussen M, Pearse D, Kuan CY, Vaudano E, Behrens A, Wagner E, Flavell RA, Davis RJ, Herdegen T. Specific pathophysiological functions of JNK isoforms in the brain. Eur J Neurosci. 2005; 21:363–377. [PubMed: 15673436]

Brown MR, Sullivan PG, Geddes JW. Synaptic mitochondria are more susceptible to Ca^{2+}overload than nonsynaptic mitochondria. J Biol Chem. 2006; 281:11658–11668. [PubMed: 16517608]

Cui H, Hayashi A, Sun HS, Belmares MP, Cobey C, Phan T, Schweizer J, Salter MW, Wang YT, Tasker RA, Garman D, Rabinowitz J, Lu PS, Tymianski M. PDZ protein interactions underlying NMDA receptor-mediated excitotoxicity and neuroprotection by PSD-95 inhibitors. J Neurosci. 2007; 27:9901–9915. [PubMed: 17855605]

Author Manuscript Author Manuscript Author Manuscript Author Manuscript

DeRidder MN, Simon MJ, Siman R, Auberson YP, Raghupathi R, Meaney DF. Traumatic mechanical injury to the hippocampus in vitro causes regional caspase-3 and calpain activation that is influenced by NMDA receptor subunit composition. Neurobiol Dis. 2006; 22:165–176. [PubMed: 16356733]

Faden AI, Lemke M, Simon RP, Noble LJ. *N*-methyl-D-aspartate antagonist MK801 improves outcome following traumatic spinal cord injury in rats: behavioral, anatomic, and neurochemical studies. J Neurotrauma. 1988; 5:33–45. [PubMed: 3057216]

Frizelle PA, Chen PE, Wyllie DJ. Equilibrium constants for (R)-[(S)-1-(4- bromo-phenyl)-ethylamino]-(2,3-dioxo-1,2,3,4-tetrahydroquino xalin-5-yl)- methyl]-phosphonic acid (NVP-AAM077) acting at recombinant NR1/NR2A and NR1/NR2B *N*-methyl-D-aspartate receptors: implications for studies of synaptic transmission. Mol Pharmacol. 2006; 70:1022–1032. [PubMed: 16778008]

Gascon S, Sobrado M, Roda JM, Rodriguez-Pena A, Diaz-Guerra M. Excitotoxicity and focal cerebral ischemia induce truncation of the NR2A and NR2B subunits of the NMDA receptor and cleavage of the scaffolding protein PSD-95. Mol Psychiatry. 2008; 13:99–114. [PubMed: 17486105]

Geddes-Klein DM, Serbest G, Mesfin MN, Cohen AS, Meaney DF. Pharmacologically induced calcium oscillations protect neurons from increases in cytosolic calcium after trauma. J Neurochem. 2006; 97:462–474. [PubMed: 16539664]

Haeusgen W, Boehm R, Zhao Y, Herdegen T, Waetzig V. Specific activities of individual c-Jun N-terminal kinases in the brain. Neuroscience. 2009; 161:951–959. [PubMed: 19364525]

Hardingham GE, Arnold FJ, Bading H. Nuclear calcium signaling controls CREB-mediated gene expression triggered by synaptic activity. Nat Neurosci. 2001; 4:261–267. [PubMed: 11224542]

Hardingham GE, Bading H. Synaptic versus extrasynaptic NMDA receptor signalling: implications for neurodegenerative disorders. Nat Rev Neurosci. 2010; 11:682–696. [PubMed: 20842175]

Hardingham GE, Fukunaga Y, Bading H. Extrasynaptic NMDARs oppose synaptic NMDARs by triggering CREB shut-off and cell death pathways. Nat Neurosci. 2002; 5:405–414. [PubMed: 11953750]

Harney SC, Jane DE, Anwyl R. Extrasynaptic NR2D-containing NMDARs are recruited to the synapse during LTP of NMDAR-EPSCs. J Neurosci. 2008; 28:11685–11694. [PubMed: 18987204]

Johnson PR, Tepikin AV, Erdemli G. Role of mitochondria in Ca(2+) homeostasis of mouse pancreatic acinar cells. Cell Calcium. 2002; 32:59–69. [PubMed: 12161106]

Liu Y, Wong TP, Aarts M, Rooyakkers A, Liu L, Lai TW, Wu DC, Lu J, Tymianski M, Craig AM, Wang YT. NMDA receptor subunits have differential roles in mediating excitotoxic neuronal death both in vitro and in vivo. J Neurosci. 2007; 27:2846–2857. [PubMed: 17360906]

Lusardi TA, Rangan J, Sun D, Smith DH, Meaney DF. A device to study the initiation and propagation of calcium transients in cultured neurons after mechanical stretch. Ann Biomed Eng. 2004; 32:1546–1558. [PubMed: 15636114]

Monyer H, Burnashev N, Laurie DJ, Sakmann B, Seeburg PH. Developmental and regional expression in the rat brain and functional properties of four NMDA receptors. Neuron. 1994; 12:529–540. [PubMed: 7512349]

Naga KK, Sullivan PG, Geddes JW. High cyclophilin D content of synaptic mitochondria results in increased vulnerability to permeability transition. J Neurosci. 2007; 27:7469–7475. [PubMed: 17626207]

Neyton J, Paoletti P. Relating NMDA receptor function to receptor subunit composition: limitations of the pharmacological approach. J Neurosci. 2006; 26:1331–1333. [PubMed: 16452656]

Nikolaidis, N.; Pitas, I. 3-D Image Processing Algorithms. John Wiley and Sons; New York: 2001.

Peng TI, Greenamyre JT. Privileged access to mitochondria of calcium influx through *N*-methyl-D-aspartate receptors. Mol Pharmacol. 1998; 53:974–980. [PubMed: 9614198]

Philpott KL, Facci L. MAP kinase pathways in neuronal cell death. Cns Neurol Dis-Drug Targets. 2008; 7:83–97.

Pirianov G, Brywe KG, Mallard C, Edwards AD, Flavell RA, Hagberg H, Mehmet H. Deletion of the c-Jun N-terminal kinase 3 gene protects neonatal mice against cerebral hypoxic-ischaemic injury. J Cereb Blood Flow Metab. 2007; 27:1022–1032. [PubMed: 17063149]

Author Manuscript Author Manuscript Author Manuscript Author Manuscript

Rintoul GL, Filiano AJ, Brocard JB, Kress GJ, Reynolds IJ. Glutamate decreases mitochondrial size and movement in primary forebrain neurons. J Neurosci. 2003; 23:7881–7888. [PubMed: 12944518]

Sattler R, Charlton MP, Hafner M, Tymianski M. Distinct influx pathways, not calcium load, determine neuronal vulnerability to calcium neurotoxicity. J Neurochem. 1998; 71:2349–2364. [PubMed: 9832133]

Soriano FX, Papadia S, Hofmann F, Hardingham NR, Bading H, Hardingham GE. Preconditioning doses of NMDA promote neuroprotection by enhancing neuronal excitability. J Neurosci. 2006; 26:4509–4518. [PubMed: 16641230]

Stanika RI, Pivovarova NB, Brantner CA, Watts CA, Winters CA, Andrews SB. Coupling diverse routes of calcium entry to mitochondrial dysfunction and glutamate excitotoxicity. Proc Natl Acad Sci USA. 2009; 106:9854–9859. [PubMed: 19482936]

Starkov AA, Chinopoulos C, Fiskum G. Mitochondrial calcium and oxidative stress as mediators of ischemic brain injury. Cell Calcium. 2004; 36:257–264. [PubMed: 15261481]

Thomas CG, Miller AJ, Westbrook GL. Synaptic and extrasynaptic NMDA receptor NR2 subunits in cultured hippocampal neurons. J Neurophysiol. 2006; 95:1727–1734. [PubMed: 16319212]

von Engelhardt J, Coserea I, Pawlak V, Fuchs EC, Kohr G, Seeburg PH, Monyer H. Excitotoxicity in vitro by NR2A- and NR2B-containing NMDA receptors. Neuropharmacology. 2007; 53:10–17. [PubMed: 17570444]

Waetzig V, Zhao Y, Herdegen T. The bright side of JNKs – multitalented mediators in neuronal sprouting, brain development and nerve fiber regeneration. Prog Neurobiol. 2006; 80:84–97. [PubMed: 17045385]

Waxman EA, Lynch DR. *N*-methyl-D-aspartate receptor subtypes: multiple roles in excitotoxicity and neurological disease. Neuroscientist. 2005; 11:37–49. [PubMed: 15632277]

Weitlauf C, Honse Y, Auberson YP, Mishina M, Lovinger DM, Winder DG. Activation of NR2A-containing NMDA receptors is not obligatory for NMDA receptor-dependent long-term potentiation. J Neurosci. 2005; 25:8386–8390. [PubMed: 16162920]

Yang DD, Kuan CY, Whitmarsh AJ, Rincon M, Zheng TS, Davis RJ, Rakic P, Flavell RA. Absence of excitotoxicity-induced apoptosis in the hippocampus of mice lacking the Jnk3 gene. Nature. 1997; 389:865–870. [PubMed: 9349820]

Zhao J, Peng Y, Xu Z, Chen RQ, Gu QH, Chen Z, Lu W. Synaptic metaplasticity through NMDA receptor lateral diffusion. J Neurosci. 2008; 28:3060–3070. [PubMed: 18354009]

Author Manuscript Author Manuscript Author Manuscript Author Manuscript

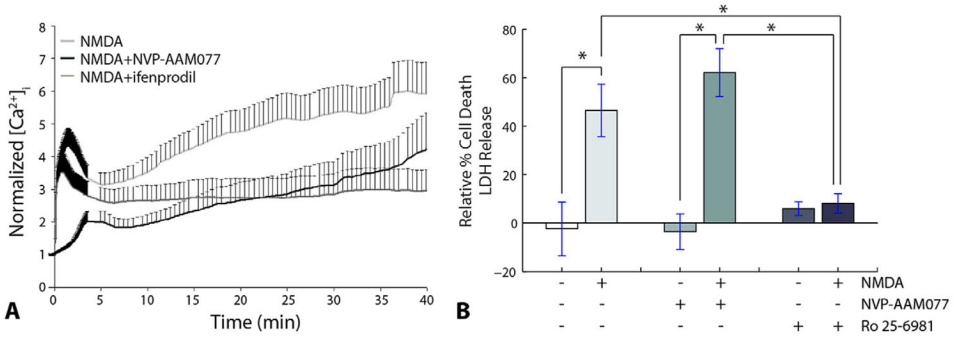

Fig. 1.

Calcium signaling, and neuronal death following NMDA receptor activation. (A) Cultures were treated with 100 μM NMDA (with 10 μM glycine) and Fura-2 imaging data showed an initial peak increase in cytosolic calcium, followed by a partial recovery and subsequent slow accumulation over the ensuing hour. Inhibiting NR2A-containing NMDARs (500 nM NVP-AAM077) attenuated the early transient increase but did not affect the long term rise in cytosolic calcium levels. In contrast, blockade of NR2B-containing NMDARs (3 μM ifenprodil) eliminated the late phase accumulation of cytosolic calcium. (B) Treatment with 30 μM NMDA caused a significant increase in neuronal death, indicated by an increase in LDH release, 23 h following the 1 h NMDA treatment. Blocking NR2A-containing NMDARs did not significantly change the neuronal viability after NMDA treatment, but inhibiting NR2B-containing NMDARs significantly reduced neuronal death to levels observed in control cultures.

Author Manuscript
Author Manuscript
Author Manuscript
Author Manuscript

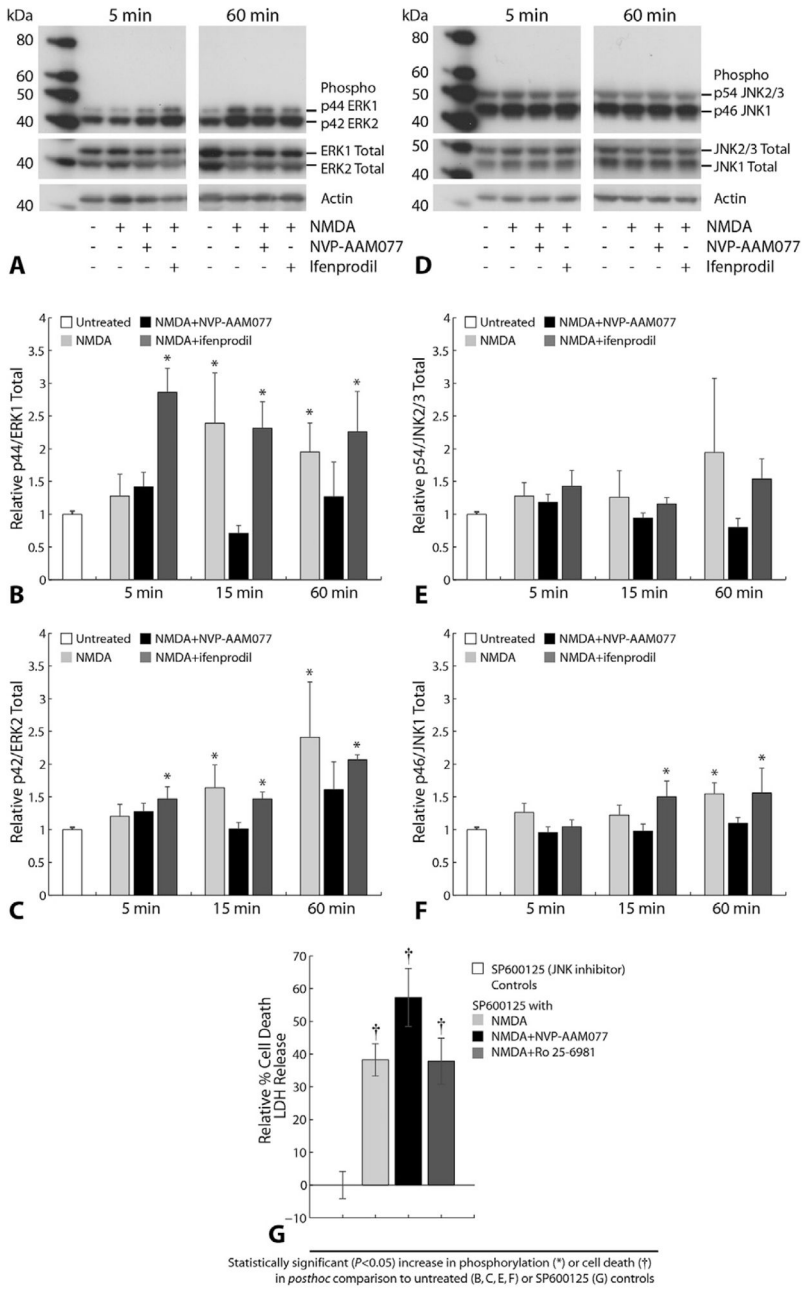

Fig. 2.

The differential activation of ERK and JNK from NMDAR subunit activation, and its role in mediating neuronal death. Mitogen activated protein kinase (MAPK) for early response kinase (ERK) and c-jun N terminal kinase (JNK) are elevated following NMDA stimulation (100 μM). Representative western blots and densitometry quantifications are shown for ERK (A–C) and JNK (D–F) activation following NMDA stimulation. Inhibiting NR2A-containing NMDARs led to a significant decrease in both 42 and 44 kDa ERK phosphorylation (B and C). Inhibition of NR2A-containing NMDARs also significantly reduced 46 kDa JNK phosphorylation levels to control levels; cultures treated with an NR2B-containing NMDAR

antagonist were not significantly different from NMDA treated cultures (F). (G) NMDA (30 μM) causes a significant increase in LDH release. Inhibiting JNK phosphorylation with 20 μM SP600125 led to a loss in the neuroprotection offered by NR2B antagonism in Fig. 1B.

Author Manuscript Author Manuscript Author Manuscript Author Manuscript

Author Manuscript Author Manuscript Author Manuscript Author Manuscript

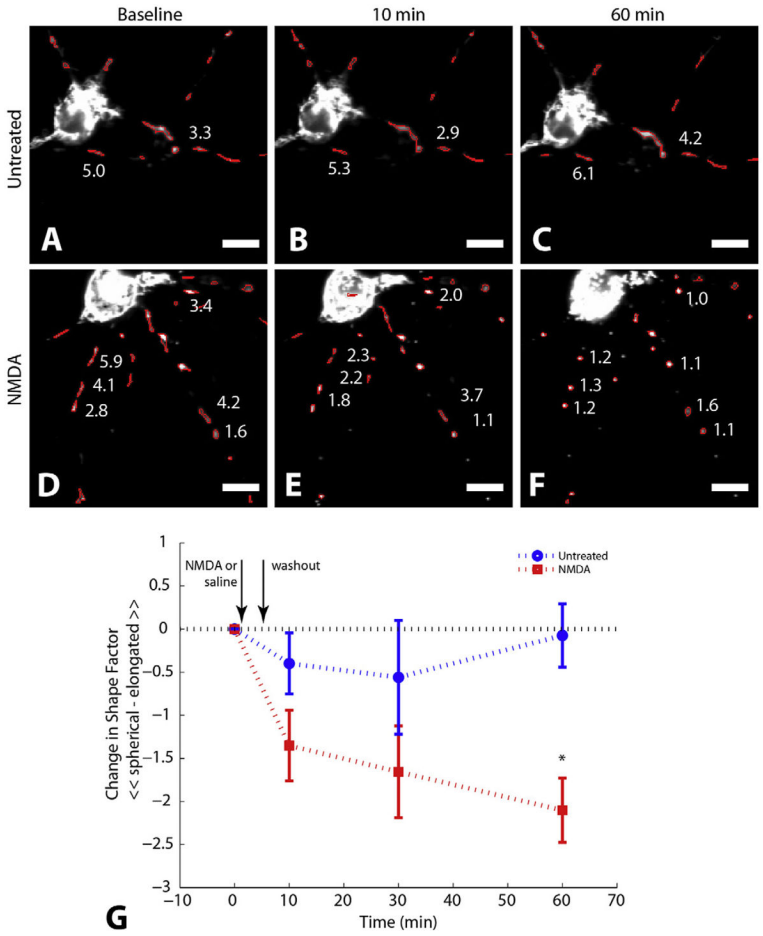

Fig. 3.

Mitochondria morphology changes following NMDA stimulation. (A–F) Primary cortical neurons were transfected with an eYFP-cytochrome C construct to label individual mitochondrion. Automated image processing yielded a shape index (SI), defined as the maximum length to width, for each outlined mitochondrion. Numbers in each image indicate the shape factor associated with different mitochondria. In the absence of any stimulation, mitochondrion shape index remains stable over time (A–C). In comparison, 5 min of NMDA treatment (100 μMNMDA + 10 μMglycine) causes a noticeable contraction of mitochondria that persists as long as 1 h following stimulation (D–F). (G) The change in the shape factor of each mitochondrion showed differences between NMDA treatment and untreated cultures 10 min after the start of the experiment, and these differences were significantly different 1 h after treatment, indicating the transient stimulation caused a permanent change in mitochondria morphology. The temporary perturbation in the shape factor of untreated cells is attributed by the mechanical disturbance during washout. Scale bars 10 μm.

Author Manuscript Author Manuscript Author Manuscript Author Manuscript

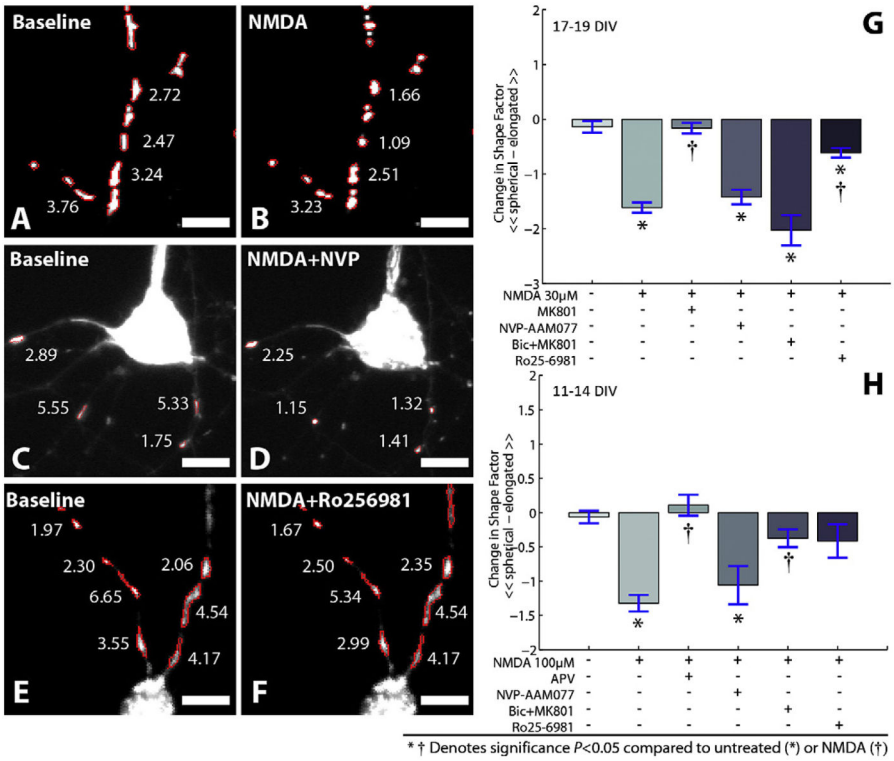

Fig. 4.

Changes in mitochondria morphology are influenced by NMDAR subunit activation. (A–F) 10 min following NMDA treatment, mitochondrion shape index decreases (A and B). The relative amount of change in mitochondria shape is maintained if the NR2A-containing NMDARs are inhibited prior to NMDA treatment (C and D). Alternatively, the shape of mitochondria is preserved by blocking NR2B containing NMDARs (E and F). (G) Significant differences in the shape factor (ΔSI), defined as the difference between pre-NMDA and post-NMDA shape measures for individual mitochondrion, were observed following NMDA treatment and were not significantly altered when NR2A-containing NMDARs were inhibited. Change in shape of mitochondria was significantly reduced in cultures when NR2B-containing NMDARs were inhibited. Blocking synaptic NMDARs with a pretreatment of bicuculline (Bic) + MK801 treatment did not prevent mitochondrial swelling in mature cultures (G) but significantly reduced swelling in younger cortical cultures (H). *NVP* in micrographs denote NVP-AAM077. Scale bars 10 µm.

Author Manuscript Author Manuscript Author Manuscript Author Manuscript

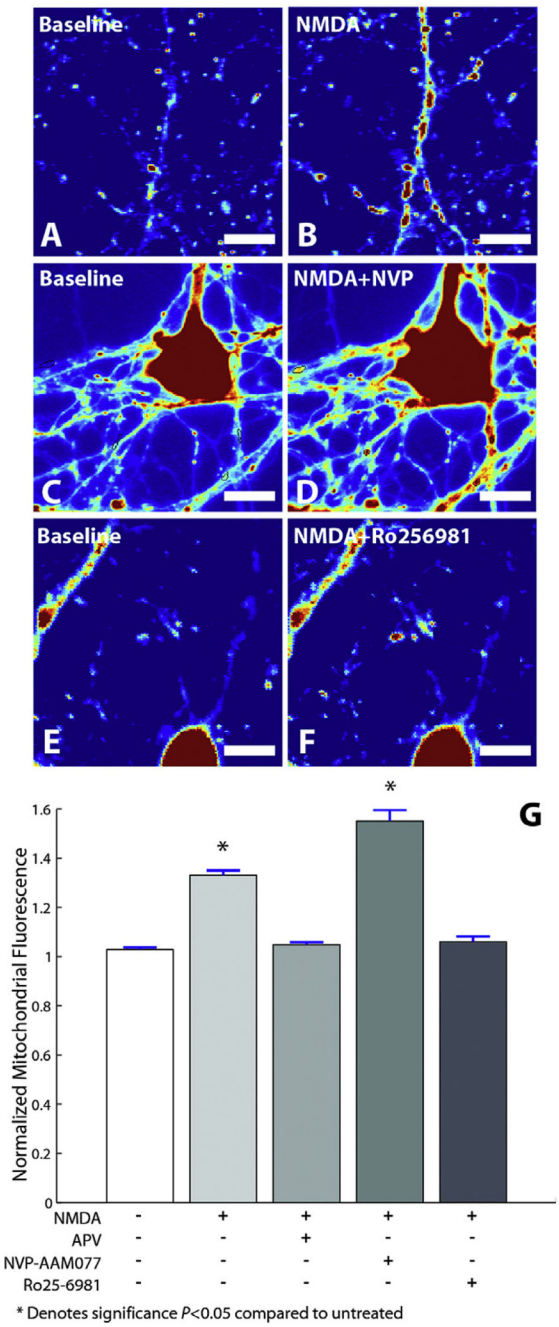

Fig. 5.

Calcium accumulation in the mitochondria is controlled by the activation of NR2B containing NMDARs. Rhod-2 labeled primary neurons were stimulated with NMDA (100 μM) and eYFP labeled mitochondria images were superimposed on the Rhod-2 images to estimate mitochondrial calcium. NMDA treatment caused a significant increase in normalized fluorescence (A and B) and this increase was enhanced further with the inhibition of NR2A-containing NMDARs (C and D). In the presence of the NR2B

antagonist Ro 25-6981, NMDA treatment did not cause a significant increase in normalized fluorescence (E and F). (G) NVP in micrographs denote NVP-AAM077. Scale bars 10 μm.

Author Manuscript Author Manuscript Author Manuscript Author Manuscript

Author Manuscript Author Manuscript Author Manuscript Author Manuscript

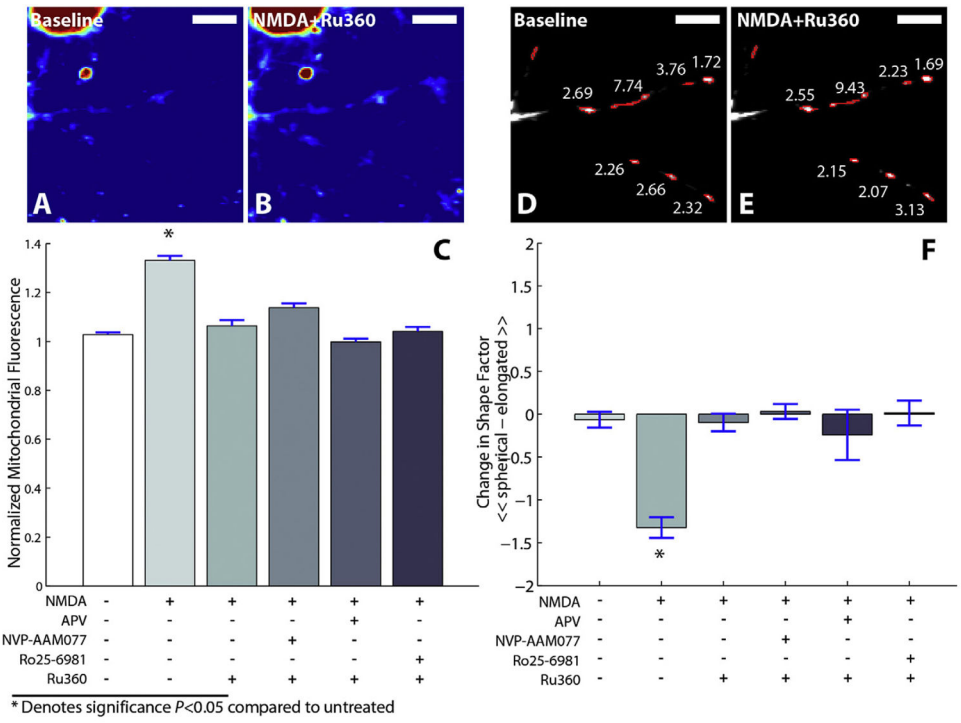

Fig. 6.

Calcium accumulation in the mitochondria is caused by enhanced uniporter uptake and is associated with morphological swelling. Using Rhod-2 fluorescence changes as an indicator of mitochondrial calcium (A and B), normalized changes in fluorescence following NMDA (100 μM) treatment were significantly reduced by inhibiting the mitochondria uniporter uptake with Ru360 (C). Inhibiting the mitochondria calcium uniporter eliminated changes in morphology with NMDA treatment (D–F, $P > 0.05$ compared to untreated controls). Scale bars 10 μm.